Microchemical Journal 214 (2025) 113994

Contents lists available at ScienceDirect

Microchemical Journal

journal homepage: www.elsevier.com/locate/microc

Review Article

Strategies for analysing hyperspectral imaging data for food quality and safety issues – A critical review of the last 5 years

Miriam Medina–García [a], José M. Amigo [b,c], Miguel A. Martínez-Domingo [d], Eva M. Valero [d], Ana M. Jiménez–Carvelo [a,*]

[a] Department of Analytical Chemistry, Faculty of Sciences, University of Granada, Av. Fuentenueva s.n., 18071 Granada, Spain
[b] Department of Analytical Chemistry, University of the Basque Country UPV/EHU, 48080, Bilbao, P.O. Box 644, Basque Country, Spain
[c] IKERBASQUE, Basque Foundation for Science, 48011 Bilbao, Spain
[d] Department of Optics, Faculty of Sciences, University of Granada, Av. Fuentenueva s.n., 18071 Granada, Spain

ARTICLE INFO

Keywords:
Food quality
Food safety
Hyperspectral imaging
Chemometrics
Analytical chemistry

ABSTRACT

Hyperspectral imaging is now establishing itself as a transformative analytical technique in the food safety and quality domains, offering unique capabilities for non-destructive, real-time, and high-resolution analysis of food at different levels of its production. Hyperspectral imaging combines the strengths of computer vision and classical spectroscopy. It provides both spatial and spectral information, making it a powerful and green alternative to the conventional techniques employed in this field.

This critical review explores the advances in hyperspectral imaging applications, highlighting its potential to revolutionize food quality and safety assessment, including adulteration, contamination and non-conformity detection. Recent breakthroughs in sensor technology, data processing algorithms, and machine learning integration are discussed, emphasizing the most popular data analysis strategies and their role in addressing the challenges of complex food matrices and dynamic production environments. This review underlines the data analysis approaches applied in each of the collected works, highlighting two trends: studying food samples as a whole or analyzing them as a set of pixel-spectra. Machine learning methods such as principal component analysis, partial least squares regression, partial least squares discriminant analysis, soft independent modelling of class analogy, and support vector machines have been widely applied for the analysis of food samples. These techniques are used for both qualitative and quantitative purposes, regardless of the sample's origin (plant- or animal-based) or its complexity. Additionally, this review outlines the limitations of hyperspectral imaging, such as high costs, computational demands, and the need for standardized protocols, while identifying opportunities for future research and industrial implementation.

1. Introduction

Food quality and safety are two fundamental pillars of the food production and processing chain. According to the Food and Agriculture Organization (FAO) of the United Nations, food safety aims to ensure that foodstuffs are free of possible toxic or hazardous substances that could cause harm to human health if consumed [1]. Therefore, explaining the concepts of toxicity and hazard is essential to understand food safety. Toxicity is defined as the capacity of a substance present in food to produce harm or injury in humans under any condition. In contrast, hazard is the probability of this substance causing harm or injury to humans when it is present in an unsafe form or quantity. Hazardous materials can be physical, chemical, biological, or allergenic. Physical hazards include physical materials not normally found in food, such as stones, bones, and bolts, which cause illness or injury. Chemical hazards are substances that could be intentionally or unintentionally added to food products and are harmful to health. This is the case with pesticides, toxic metals or, for instance, certain additives [2]. On the other hand, biological hazards refer to living organisms, including microorganisms, associated with food that can cause diseases (like bacteria, viruses, worms, or insects) [3]. Lastly, it is also important to address allergens, which are substances that can trigger allergic reactions upon contact with the human body [4].

Food quality is defined by the attributes or characteristics of food

* Corresponding author.
E-mail address: amariajc@ugr.es (A.M. Jiménez–Carvelo).

https://doi.org/10.1016/j.microc.2025.113994
Received 25 February 2025; Received in revised form 24 April 2025; Accepted 15 May 2025
Available online 17 May 2025

products that influence their value and, consequently, their acceptability to consumers. These attributes include nutritional values, organoleptic and physicochemical parameters, and functional properties [5]. Therefore, food safety can be considered a key element of food quality. Note that food quality and food safety terms can be brought together in what is known as food fraud. On the one hand, according to some authors, food fraud comprises adulteration, misrepresentation (e.g. counterfeiting) as well as theft, tampering, diversion, tax evasion, grey market and overrun [6]. On the other hand, the European Union legislation does not provide a definition of food fraud, even though Commission Regulation (EU) No 2019/1715 provides key elements to define food fraud. Thus, food fraud can be defined as non-compliance including any suspected intentional action by businesses or individuals to deceive purchasers with a view to increase their profits [7]. Food fraud not only misleads consumers but can also compromise consumers' health, causing illness or even death. According to the June 2024 summary of articles on food fraud, published by the European Commission, 30 food fraud cases were reported in the world in that month alone [8]. Among them, it is worth mentioning the case in India, where the adulteration of a spirit with methanol led to 25 deaths and over 60 hospitalizations. This is just one example that underscores the need to establish control measures and mechanisms to combat food fraud and protect consumers.

The taxonomy of food fraud usually comprises three main categories: adulteration, non-conformity and contamination. The first one encompasses all intentional alterations of a food product by adding or substituting ingredients that modify its intrinsic properties and mislead consumers. Generally, this practice reduces costs and increases profits using lower quality or non-permitted ingredients. A common example is diluting expensive products, such as edible oils or spirits, with cheaper substances not originally present in them. On the other hand, non-conformity fraud implies that a food product does not comply with established regulations or specifications, whether in terms of labelling, composition, or production processes. It may occur unintentionally to defraud, but it still affects the quality and/or safety of the product. Finally, food contamination fraud occurs when harmful or hazardous substances are intentionally or accidentally present in food, thereby affecting consumer safety and integrity. This practice may have malicious intent or result from negligent practices [9,10].

In the fight against food fraud, a wide range of analytical methods have been developed to ensure food quality and safety. Some of the techniques used are (i) spectroscopic such as nuclear magnetic resonance or infrared, (ii) biological such as biosensors and (iii) separation such as chromatography or electrophoresis. Among them, methods based on chromatographic techniques, such as gas chromatography and high-performance liquid chromatography, are the most widely used for detection of several types of contaminants and residues [11]. These techniques are accurate and highly sensitive, but they have some weaknesses, such as being destructive, requiring complex sample pretreatment, skilled professionals, expensive and sophisticated equipment, and long analysis times. [12]. To address these shortcomings, optical sensing techniques such as hyperspectral imaging (HSI) and imaging spectroscopy have emerged as viable alternatives in food quality control [13].

HSI integrates imaging and spectroscopy, combining the advantages of both technologies into a rapid, non-destructive, and environmentally friendly technique. The origins of HSI date back to the 1970s and 1980s, when mineral mapping began, and airborne imaging spectrometry (AIS) was developed [14]. Since then, its applications have grown beyond remote sensing, extending into fields like environmental science, pharmaceutical and medical fields, and the food industry, among others [15–17]. HSI involves the acquisition of an image of a material system at different spectral bands, simultaneously providing spatial and spectral information about the material. It provides information on the physical and geometrical characteristics of the material, including size, shape, spatial distribution, and appearance. Additionally, spectral data can reveal insights into its chemical composition [18].

However, although this dual capability positions HSI as a highly versatile analytical tool, it also introduces significant complexity. High-dimensional datasets require sophisticated preprocessing, calibration, and multivariate analysis techniques, which may hinder usability for non-experts or small-scale operations. Furthermore, the effectiveness of HSI relies heavily on the proper alignment between the sensor's spectral range and the specific chemical markers (such as absorption bands) of interest—an aspect often underreported or assumed in many applications. These factors underscore the importance of methodological guidance in selecting suitable hardware and analytical strategies, particularly in food-related studies where sample diversity and matrix complexity are substantial.

The fundamental principle of HSI is based on the interaction between light and matter. When a material system is exposed to electromagnetic radiation with specific characteristics, it interacts with the radiation, causing changes in the radiation that relate to the physical and chemical properties of the material. These changes can be detected, recorded, and represented visually as an image. The images are divided into spatial units called pixels. In HSI, each pixel contains a "spectral fingerprint" that enables the identification and characterization of this spatial point in the material system [19]. This pixel-level spectral analysis makes HSI a powerful tool for enhancing both the quality control and safety verification of food products, in addition to offering the advantage of studying the food without physical contact. These capabilities have been showcased in numerous studies for assessing the quality of natural food such as fruits, cereals, meats [20–22] and processed foods such as, bread and cheese [23,24]. A search in the Scopus database using the keywords "Food", "Quality", "Safety", and "Hyperspectral imaging" (see Fig. 1) revealed a total of 250 publications over the past 10 years (up to 2024). This indicates a growing interest in the application of HSI in the field of analytical food chemistry. While this review focuses on recent advancements (over the last 5 years), the trend highlights the increasing adoption and exploration of this technique as a transformative tool in food quality and food safety control.

The available literature offers a limited number of review articles that focus on the evaluation of food products using HSI. Specifically, only eight scientific studies devoted to this topic have been found, including six systematic reviews [25–30], one book chapter [31], and one entire handbook [32]. As a complement to the broader scope reviews on HSI applications in this field, other studies have focused on its use in specific food products. For instance, Wang et al. [33] evaluated the advancements, limitations, and challenges of HSI to assess wheat quality. Furthermore, Peraza-Alemán et al. [34] reviewed its application in potatoes, Li et al. [35] in different fruit and vegetable products, Ismail et al. [36] in seafood products and Matenda et al. [37] in meat.

However, despite acknowledging the value and potential of HSI

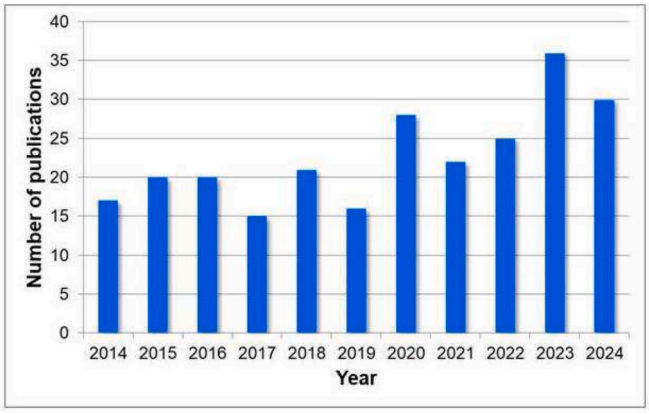

Fig. 1. Temporal distribution of published studies about food quality and safety control using HSI. Information collected from Scopus database.

combined with machine learning for food evaluation, many studies fall short of addressing fundamental aspects that are critical when selecting and applying this analytical technique. A recurring weakness is the lack of detail regarding the specific signal extraction strategy, i.e., how the chemical information of interest is isolated from the hyperspectral data cube. This omission is not trivial. The quality and relevance of the extracted signal directly influence the performance of multivariate models developed using chemometric tools, such as partial least squares discriminant analysis (PLS-DA) or support vector machines (SVM), among others.

Given that HSI inherently produces high-dimensional datasets, decisions around dimensionality reduction methods, signal preprocessing, and region of interest (ROI) selection are crucial. Yet, these methodological choices are often underreported or based on convenience rather than experimental justification. This lack of transparency can limit reproducibility and hinder cross-study comparisons. Moreover, the selection of the data analysis strategy should be strongly guided by the nature of the food matrix (homogeneous or heterogeneous) [38], and the specific analytical objective, such as detection, classification, or quantification. Unfortunately, few studies provide a rationale for their chosen approach, leading to a disconnect between the technique's theoretical potential and its practical application in real-world scenarios.

In this context, the present review aims to fill this gap by providing the scientific community and industry experts with a detailed analysis of the types of foodstuffs that can be analyzed using HSI. It also identifies the most appropriate analytical signal to capture the chemical information of interest for food evaluation. In this regard, the review is structured into four sections following this introductory section on the state of the art: (i) Core concepts of HSI. (ii) Strategies for extracting and analysing target information. (iii) Overview of studies published in the last five years using HSI to assess food quality focusing on what type of analytical signal has been used. (iv) Conclusions and challenges to be addressed.

2. Core concepts of hyperspectral imaging

HSI can be understood from a global perspective as a set of capture and image processing techniques. These techniques allow users to access any spectral magnitude that can be captured by a camera (that is, a magnitude dependent on the wavelength of radiation). As an imaging technique, its primary advantage over area-based spectral information devices, such as spectrophotometers or spectroradiometers, is that it can capture spectral data on a pixel-by-pixel basis within an image. The spatial resolution is typically much higher than that of typical spectrometers, and it is constrained by the distance to the material, as well as the capabilities of the optics and sensor. Therefore, an HSI device yields a set of spectral fingerprints within the same measurement area, whereas an area-based device yields only one spectrum.

When comparing HSI with a Red, Green, and Blue (RGB) camera, one of the main differences is the size of the final image data for the same number of pixels in both systems. HSI images are normally referred to as a "hyperspectral cubes", even though they are not true cubes in a geometric sense, hence they could be termed a "hyperspectral (pseudo) cube". A more precise definition is a data array with two spatial dimensions and one spectral dimension. This is because, after post-processing, each spectral band becomes a monochrome image (2D image in which horizontal and vertical dimensions correspond to the spatial content of the captured scene). If this set of images is stacked one on top of the other, ordered by increasing wavelength, a three-dimensional data structure is formed. This has been illustrated countless times and is also depicted in Fig. 2, which presents a workflow of the key steps involved in capturing a hyperspectral image [39].

An RGB camera can be seen as a specific type of HSI device with only three relatively wide spectral bands. RGB images also form 3D structures, where the three-color channels (R, G, and B bands) are stacked together. Nevertheless, RGB devices are not typically considered in the same category as HSI.

The spectral magnitude that is directly measured by an HIS camera is usually the spectral radiance. If this is the case, the device produces radiance cubes or simply rad cubes [40]. Radiance can be mathematically transformed into reflectance (reflectance cubes), absorbance, transmittance, or interactance [41]. For some systems, it is also possible to access the raw sensor response data (raw cubes), interesting for in specific application cases generally in controlled environments.

The incoming radiation is split into different spectral bands (either by a diffraction-based dispersing device, by an array of filters incorporated into the sensor or other techniques) and then focused onto the

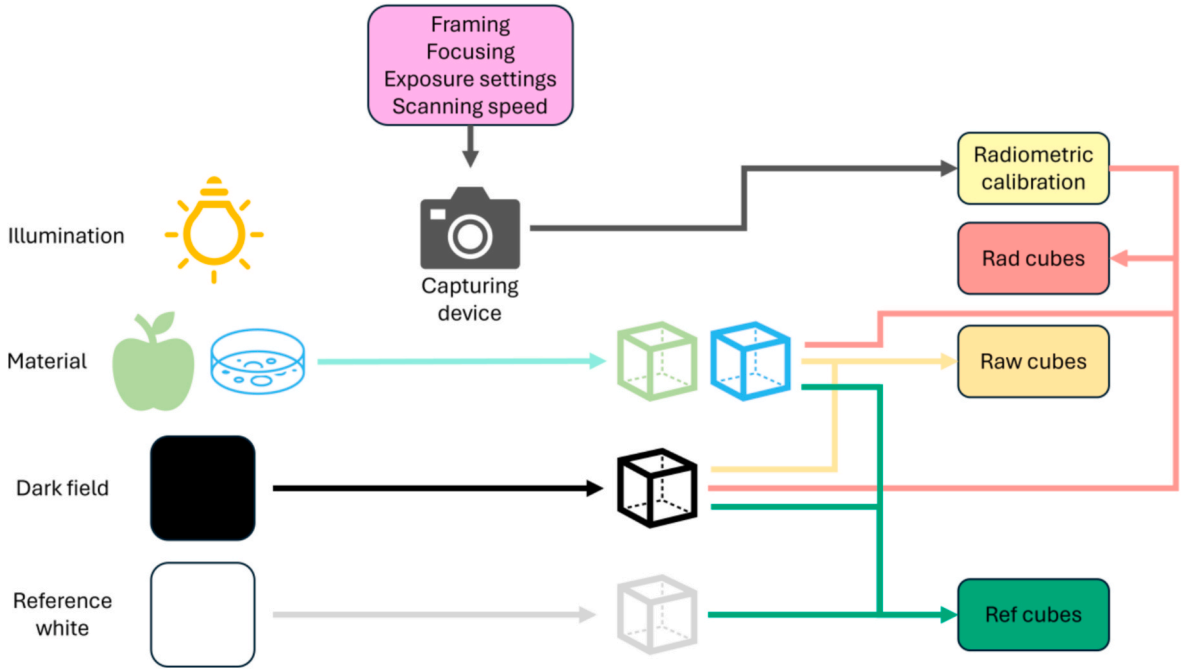

Fig. 2. Overview of the main data processing steps for generating a hyperspectral image in HSI capture devices.

sensor [42]. The capture setup varies depending on the magnitude being measured; however, there are essential steps common to every spectral capture, including calibration, raw data capture, and post-processing to obtain the final set of pixel-wise spectra. The calibration step aims to gather sufficient information about the spectral distribution and spatial inhomogeneity of the light source, as well as the dark current noise, to correct for these effects in the captured image data. Therefore, it must be performed each time the device setup is altered. It is advisable to calibrate at least once at the beginning and once at the end of each capture session. Besides this setup and noise-dependent calibration, the manufacturer may perform an additional intrinsic radiometric calibration, enabling the device to retrieve radiance data (rad cubes) from the raw sensor response data cubes [43]. The raw data are mediated by the sensor spectral response and include several sources of noise that naturally occur in the HSI. Nevertheless, as mentioned before, they may still provide sufficient information to be useful in certain applications.

Spatial resolution is usually one of the key features considered in any imaging device. If the limitation by diffraction is not considered, the higher the number of pixels in the image, the higher the spatial resolution the capture system has for a fixed sensor size. Spatial resolution is therefore linked to the pixel size: smaller pixels result in higher spatial resolution [44]. However, since the optical elements that form the image on the sensor are limited by diffraction, a fine balance must be achieved between the diffraction resolution limit and pixel size. If the sensor has a very small pixel size but the optics are not adequate to exploit this design, optical aberrations and diffraction will limit the image quality. Conversely, if the optics are well-designed but the sensor has overly large pixels, the effort in designing the optics will be wasted, as the system's resolution will be constrained by the sensor [45].

Another important consideration is the spectral range covered by the HSI system. Most spectral capture devices cover the visible and near-infrared (Vis-NIR) range, roughly from 380 to 1000 nm. However, there are devices with extended ranges in the near-ultraviolet (NUV). These start mostly from 315 nm (although some specialized systems go as low as 200 nm). In the short-wavelength infrared (SWIR) range, systems operate from 900 to 1700 nm or even up to 2500 nm. The penetration depth of the radiation within the material depends on the radiation-matter interaction processes that take place and the spectral range. The NUV and Vis radiation is typically strongly absorbed by pigments, chromophores and water, while the SWIR penetrates more, although it can also be absorbed to a certain extent by water and other organic compounds. This fact turns out useful for spectroscopy applications.

Most HSI cameras are designed to capture reflectance, including both specular and diffuse components. The exclusion of the specular component can be achieved by using additional optical elements, such as polarizers, or by optimizing the illumination-observation geometry.

In hyperspectral imaging devices, in addition to spatial resolution limitations and spectral range, the spectral resolution must also be considered. This refers to the minimum wavelength separation that the system can resolve. For most hyperspectral devices, the average spectral resolution ranges from 2 to 4 nm. The spectral resolution is limited by both the physical components responsible for spectral separation and the characteristics of the sensor. For example, if the device includes a diffraction grating, the separation between the grooves must be sufficient to project the image of two distinct but adjacent wavelengths onto different pixels of the sensor. This is commonly the case with push-broom line scanners. [42].

Usually, operating the system close to the spectral and spatial resolution limits will result in the presence of noise in the image. It is often worth sacrificing some spatial or spectral resolution to reduce capture noise. This can be done through simple operations, such as averaging across pixels or adjacent wavelengths in the spectrum, so that the captured signal becomes smoother, and the noise is averaged out. This practice is called spatial or spectral "binning", and it is illustrated in Fig. 3 [46].

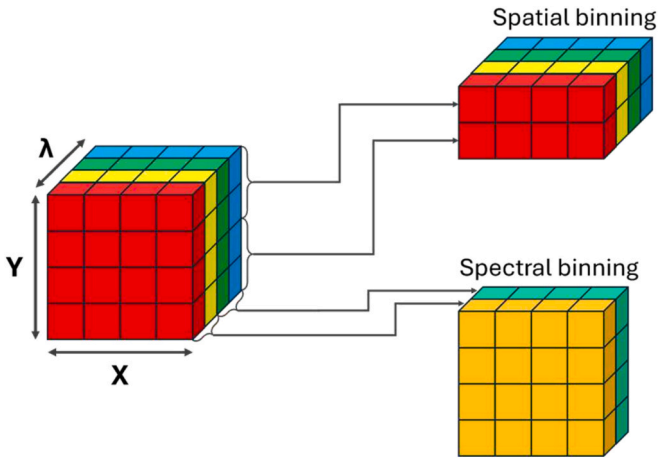

Fig. 3. Illustration of spatial and spectral binning procedures used for noise reduction in hyperspectral images.

2.1. HSI device architectures

HSI systems can be classified into five main categories based on the principle of their image acquisition design [47,48]:

1) Push-broom (line-scanning): captures one spectral line per frame using a 2D sensor, requiring scene or camera movement. It offers high spatial and spectral resolution but is best suited for static scenes.
2) Snapshot (one-shot): uses microlens arrays and filters to capture the full spectral cube in one frame. This allows the capture of dynamic scenes at the cost of reduced spatial and spectral resolution. It is a typical architecture for multispectral capture devices (typically with considerably less spectral resolution than hyperspectral devices).
3) Whisk-broom (point-scanning): Captures one or a few pixels at a time using a line sensor. Some advantages and drawbacks are shared with the push-broom architecture, although whisk-broom devices can reach very high spectral and spatial resolutions at the cost of longer capture times.
4) Spectral scanning: Acquires the entire scene for one spectral band at a time. Filtering can be achieved mechanically (interchangeable interference filters), using tunable filters such as liquid crystal tunable filters (LCTF) or acousto-optic tunable filters (AOTF); or via sequential illumination (also called illumination multiplexing) with narrowband light sources (e.g., tuneable light emitting diodes (LEDs)). This was one of the earliest HSI architectures [49,50].
5) Coded aperture: Uses a mask at the system's entrance pupil to encode spatial and spectral information into a single image. Computational algorithms such as compressed sensing, matrix factorization, Bayesian approaches like expectation maximization or deep learning-based methods are then required to reconstruct the hyperspectral cube. These devices are relatively inexpensive and allow real-time capture of dynamic scenes but require significant computational resources [51].

2.2. Data processing and storage

Regardless of the acquisition method, common data processing steps include calibration (e.g., flat-field correction, white and dark reference corrections) and format conversion, depending on the software used. Common hyperspectral cube formats include ENVI (.hdr,.img), GeoTIFF (.tif), and HDF5, with band interleaved by line (BIL), by pixel (BIP), or sequential (BSQ) storage structures [52].

After the cube is stored, some of the data correction steps can still be performed if they were not executed by the capturing software. The post-processing stage can start once the data is stored in its final form.

Depending on the application, it can involve extracting regions of interest (ROIs) either manually or automatically, computing wavelength-dependent average spectra or standard deviations across pixels, selecting spectra for classification or computing color coordinates for further analysis.

In summary, capturing spectral data requires careful consideration of various factors, including system architecture, storage format, and the software used to process the data after capture. These decisions are fundamentally 'application-dependent.

3. Target information

As mentioned in the previous sections, HSI can simultaneously obtain spatial and spectral information from a material. Spatial information can provide details about its physical characteristics, such as shape, texture, defects or irregularities, while spectral information can provide insight into its chemical composition [18]. Both forms of information can be evaluated separately or together, depending on the purpose of the study. For this reason, it is important to determine the specific scenario under which the analysis is being conducted. In this section, various scenarios are outlined according to the target information and the type of material involved.

3.1. Assessment of work scenarios for applying hyperspectral imaging in the field of food quality and safety

One of the most critical steps when considering the application of an analytical technique is evaluating the specific working scenario, and this is no different for HSI. The type of material and the required information must be carefully assessed to determine the best approach. Therefore, this section focuses on describing each scenario in detail.

3.1.1. Spatial and spectral information for food analysis

Spatial information is crucial for the real-time detection and localization of defects or irregularities, particularly in fruits and vegetables along the food production chain. These quality attributes determine the shelf life, maturity, and marketability of the product [53]. Similarly, this information can be useful for identifying the location of dispersed discernible particles in a food matrix sample or to distinguish elements with differing morphologies within it [24]. It is important to emphasize that this type of information pertains exclusively to the physical attributes of the food and its location, and it does not account for its chemical composition. This approach aligns with conventional imaging techniques, focusing solely on visual characteristics such as color, lightness, texture, shape or contour. In contrast, when aiming to determine the chemical composition of a material, spectral information is necessary.

HSI also provides spectral information for each pixel of the image. This information, combined with advanced data analysis methods, can be used to study the chemical composition of a material as a whole. It also allows for the identification of regions or particles with different compositions, and the quantification of any or all of its constituents. Its role in food quality and safety control stands out in applications such as food authentication, detection of adulterations, or contaminant identification, among others. [54].

3.1.2. Types of material and data extraction strategy

At this point, it is important to distinguish between different types of materials, as data analysis strategies vary depending on whether the material is homogeneous or heterogeneous.

Until recently, HSI has not been considered a suitable tool for evaluating liquid food [55]. However, studies in the literature have demonstrated its effectiveness in analyzing materials in both liquid and solid forms, establishing it as a versatile analytical technique in numerous food safety and quality control applications [16]. Note that both liquid and solid food samples can exhibit homogeneous or heterogeneous characteristics. Therefore, this characteristic defines the strategy for extracting useful information from the image of the material.

A homogeneous material can be defined as a system with largely uniform surface distribution of components throughout, and its properties remain consistent across it. An example of a homogeneous food sample can be olive oil. In contrast, a heterogeneous material exhibits an uneven surface distribution of components, resulting in non-uniform properties [56]. Examples include ham, pâté or natural juice. Based on the type of material, it is necessary to define an appropriate strategy for extracting useful information after applying HSI. Two main scenarios can be considered.

The first involves homogeneous materials, where relevant information can be obtained by analyzing the average spectrum of a Region of Interest (ROI). In this context, the ROI corresponds to a chemically representative area within the material. For example, when detecting and quantifying melamine in milk, hyperspectral images of milk samples in Petri dishes are acquired. The ROI is defined at the center of the sample, excluding edges or background, to focus the analysis on the target information.

The second scenario involves heterogeneous materials, where analyzing individual pixel spectra within each ROI may be necessary to capture spatial variations in composition. Based on these two scenarios, the following information extraction strategies can be defined:

(i) ROI average spectrum. Homogeneous materials exhibit a largely uniform composition and properties. Therefore, the average spectrum of the pixels within the ROI of the hyperspectral image provides representative information for the entire material. This approach reduces data volume and simplifies processing and analysis. A practical example is the classification of edible oils by geographical origin, where the material is homogeneous, and the average spectrum is both representative and distinctive. [57]. This approach comes with limitations. It inherently assumes perfect homogeneity within the ROI, which may not always be the case in real-world samples. Subtle local variations can be masked by the averaging process, especially when caused by impurities, degradation, or processing, potentially leading to the loss of relevant information. Moreover, the spatial context is entirely lost, which might be critical in applications where distribution patterns or localized anomalies carry significant meaning. In such cases, relying solely on the average spectrum may oversimplify the material's complexity. While this strategy is computationally efficient—and in some instances may even justify the use of traditional spectroscopy instead of HSI—it should be applied with caution. The decision to use an average spectrum must be supported by a thorough assessment of sample homogeneity and a clear understanding of whether spatial information is indeed irrelevant to the analytical objective.

(ii) ROI pixel-spectra. In heterogeneous materials, spatial variability in composition and physicochemical properties is often significant. As a result, a single average spectrum fails to capture the full chemical complexity of the sample. To address this, pixel-wise analysis is required. This approach enables detailed exploration of the spatial structure of the material and its local variations, often revealing features that would otherwise be lost in averaged data. While pixel-wise analysis offers a much richer understanding of the sample, it also introduces considerable challenges. The volume of data increases dramatically, making computational load and processing time important concerns. Moreover, interpreting such high-dimensional data often requires advanced chemometric tools and expertise, which may not always be accessible to practitioners. Noise and variability at the pixel level can also complicate interpretation, especially in low-signal regions or when working with imperfectly calibrated systems. Despite these challenges, this strategy takes full advantage of the spatial resolution offered by hyperspectral imaging. In contexts

where the spatial distribution of compounds is critical (e.g., detecting contaminants, characterizing tissue, or identifying material defects), pixel-wise analysis is not only valuable but often essential. Nevertheless, its implementation should be guided by a clear analytical objective and supported by robust preprocessing and validation methods to ensure meaningful results.

Additionally, a third strategy applies to a specific type of heterogeneous material: one that consists of a homogeneous matrix with discernible particles dispersed within it. These materials are characterized by an overall uniform composition, while containing distinct particles that differ in size, shape, or composition. These particles are embedded in the matrix without significantly affecting its homogeneity. In contrast, truly heterogeneous materials exhibit broader compositional or structural variations, resulting in a non-uniform matrix. Distinguishing between these two types requires prior knowledge or clear evidence of the material's nature. A representative example is wholemeal flour. Both white and wholemeal flours share the same homogeneous matrix—mainly composed of ground endosperm—but wholemeal flour contains additional particles from the bran and germ. In this case, while the average spectrum can differentiate between white and wholemeal flour, it is insufficient to identify the type, quantity, and spatial distribution of the dispersed particles [24].

It is important to note that the spatial resolution must be smaller or equal to the particle size to detect dispersed particles. This scenario presents unique challenges. While averaging may provide a general characterization, it risks masking the contribution of minor yet potentially important constituents. Pixel-wise analysis can offer deeper insight; however, its effectiveness depends on having sufficient spatial resolution. Otherwise, the signal from the particles may blend with that of the matrix, leading to inaccurate or diluted interpretations. Therefore, for materials with dispersed particles, the analytical approach must balance spectral simplification with spatial resolution. Techniques such as segmentation, object-based analysis, or mixed-pixel modelling can be valuable here. Ultimately, recognizing this intermediate material structure early on is critical for selecting appropriate data processing methods and avoiding misleading conclusions based on oversimplified models.

Fig. 4 illustrates the three types of materials discussed earlier. In the first case, where the material consists of a homogeneous matrix, all pixels contain the same spectral information, so the average spectrum of the ROI is representative of the entire sample. In contrast, the other two cases involve materials with heterogeneous components: the average spectra in these cases incorporate data from pixels with different constituents (A, B, and C), each exhibiting distinct spectral characteristics. While the average spectrum can reveal differences between material samples, it does not provide information about the spatial distribution of each constituent.

Advanced data analysis techniques, such as multivariate curve resolution (MCR), can be used to estimate the contribution of each constituent based on the average spectrum. However, for materials with a homogeneous matrix containing embedded particles, the QPC (Quantification by Pixel Counting) methodology is more suitable. This approach allows for the identification and quantification of individual particles, as well as the determination of their composition [24].

3.2. Hyperspectral image data analysis

Once the working scenario is defined—that is, the material type and the target analytical feature to be determined—the next step is to extract and analyze the relevant information from the hyperspectral image data. At this stage, it is important to distinguish between qualitative and quantitative information. Qualitative information involves the

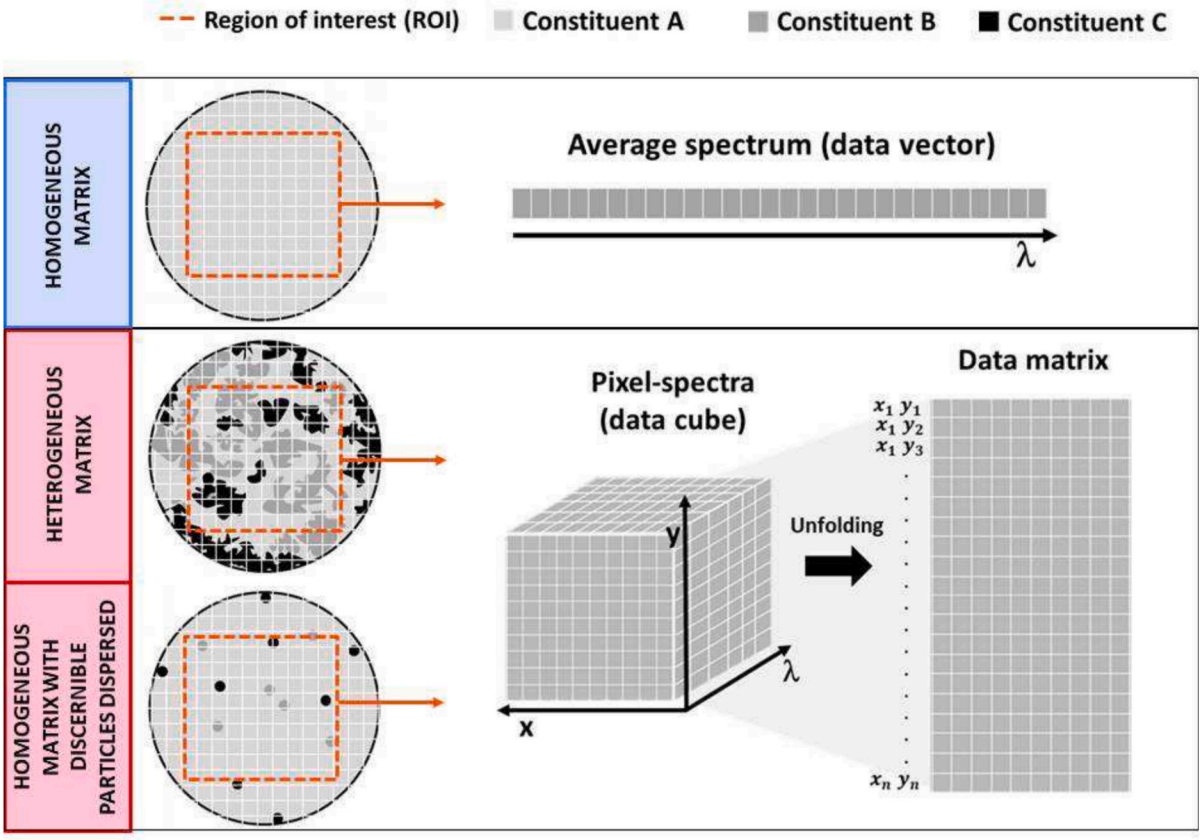

Fig. 4. Comparative representation of material types and their spectral characteristics for homogeneous and heterogeneous materials.

detection, identification, classification, or categorization of the material based on one or more distinctive features. In contrast, quantitative information focuses on determining the amount of the target features present in the material. If the objective is to obtain qualitative information about the entire sample, such as differentiating between various types of edible vegetable oils, the average spectrum may provide sufficient data. However, if the goal is to analyze specific regions of the material, a pixel-by-pixel spectral analysis may be necessary.

Chemometrics, which involves applying machine learning techniques to chemistry—including spectroscopy, chromatography, and other analytical methods—can be effective for extracting qualitative and/or quantitative information from hyperspectral image data. It can be categorized into two approaches: unsupervised and supervised methods. In the former, the model does not use class labels, and pattern recognition is employed to uncover natural groupings among the objects. In the latter, the model is constructed using prior knowledge of the class to which each object or sample belongs.

Among the most widely used techniques in hyperspectral imaging (HSI) are Principal Component Analysis (PCA) and Hierarchical Cluster Analysis (HCA). Additionally, Multivariate Curve Resolution (MCR), often used to resolve complex signals, is frequently applied in this context to reduce data volume, identify key pixels and variables, and analyze the behavior of chemical compounds in the material. Supervised methods are crucial for developing both qualitative and quantitative analytical techniques. For qualitative analysis, Partial Least Squares Discriminant Analysis (PLS-DA), Support Vector Machines (SVM), and Artificial Neural Networks (ANN) are commonly used. For quantitative analysis, Partial Least Squares Regression (PLSR), Multiple Linear Regression (MLR), and SVM/ANN regression models are the most popular [58].

To effectively apply multivariate data analysis methods to hyperspectral imaging (HSI) data, it is essential to recall how hyperspectral images are captured. As discussed in section two, hyperspectral images are stored as a 3D data structure, commonly referred to as a 'hyperspectral cube.' From this data cube, Regions of Interest (ROIs) can be selected. These steps are consistent regardless of the material type being analyzed. However, data handling diverges at this point, where the previously mentioned working scenarios come into play (see section 3.1.2). Two data analysis approaches can be adopted then: (i) treating the material as a whole, and (ii) treating the material as a collection of individual pixel spectra.

(1) Material sample as a whole. Irrespective of the material type, if the goal is to obtain general qualitative information to compare a set of material, the average spectrum of each sample may be sufficient for the analysis. It is because it provides a representative overview of their main physicochemical characteristics. In this approach, each material is represented by an average spectrum that identifies and characterizes it. To analyze a set of materials, the data are arranged in a $M \times N$ matrix using the average spectrum of each one. In this matrix M symbolizes the number of materials analyzed (number of average spectra) and N corresponds to the number of variables (wavelengths). Methods such as standard normal variation (SNV) or multiplicative scatter correlation (MSC) are usually applied to preprocess the spectra contained in the matrix. Using the preprocessed matrix as an input data set, unsupervised methods will enable us to identify behavioural patterns among materials based on spectral similarities and reveal natural groupings or clusters within them. This approach provides an initial screening analysis, offering insights into the structure and variability across materials without prior assumptions. Data analysis methods such as PCA, or HCA are usually used to this end.

Supervised methods such as PLS-DA, SVM or ANN, are applied to categorize samples according to specific target analytical features. Thus, they are also called "classification and discrimination methods". These methods build a classification model. For this purpose, they establish relationships between the spectral characteristics of the materials and a qualitative (or discrete) variable that signifies a particular class, which is defined by one or more specific target analytical features. This model is properly trained, validated, and then the outcomes are assessed by quality performance metrics for classification including sensitivity, specificity, precision and accuracy, among others [59]. After having completed these steps, the trained model can be used to predict the class of new samples.

Furthermore, supervised methods such as PLSR or SVM/ANN for regression are commonly used to estimate the quantity of one or more constituents, or to quantify a specific measurable characteristic of the material. Unlike classification methods, these techniques establish relationships between specific spectral features and a known value of the target analytical feature, thereby building a quantification model [55]. In the same way as qualitative models, quantification models are trained and validated and then, results are evaluated by calculating statistical parameters. These parameters may include coefficient of determination (R^2), root mean square of residuals (RMSE), root mean square error of prediction (RMSEP), prediction residual error square sum (PRESS) and standard error of prediction (SEP) [60].

(2) Material as a Set of Pixel-Spectra. Pixel-by-pixel analysis is most useful when analyzing heterogeneous materials or when the objective is to (a) identify the location or (b) determine the spatial distribution of specific regions or particles within a sample. As a preliminary step before applying any multivariate analysis method, all spectra within a sample ROI are arranged into a single P × N matrix. In this matrix, P represents the number of pixel spectra from the ROI, and N corresponds to the number of variables (wavelengths).

Both unsupervised and supervised methods can be applied as described earlier. However, it is important to note that in this case, the analysis focuses not on individual materials, but on individual pixel-spectrum samples from a single material. Unsupervised methods provide insights into natural groupings of pixel spectra within the material, while supervised methods can be used to discriminate between pixels with similar spectral characteristics and associate them with the target analytical feature. These analyses can also be extended to pixels from different materials by vertically concatenating their data matrices.

Additionally, in the case of a material consisting of a homogeneous matrix and discernible particles dispersed in it, the QPC methodology can be applied [24]. The QPC methodology can be summarized in two main steps. The first step involves applying supervised methods to develop a classification model. They can discriminate between (i) pixels containing spectra associated with the target particles (target class) and (ii) pixels with spectra characteristic of the homogeneous matrix without the particles (alternative class). The second step focuses on quantifying the particles by counting the pixels classified as belonging to the target class. This methodology allows for both estimating the content of discernible particles and identifying their spatial distribution. For further details, see reference [24].

Fig. 5 summarises the key aspects of the approaches to analyse hyperspectral image data described above.

4. Mining information from hyperspectral signals

This section examines studies published in the last five years that have employed HSI to address food quality and safety, with a particular focus on the detection of adulteration, contamination, and non-conformities. Additionally, it highlights the diverse applications of HSI across various food types, with emphasis on the strategies used for information mining and the machine learning techniques implemented for data analysis. To identify relevant literature, a comprehensive search was conducted using the Scopus database. The studies reviewed are summarized in Table 1. It is organized to distinguish among food categories, analytical objectives, information extraction strategies, applied machine learning algorithms, and the specific aspects of food quality or safety addressed in each study. It was found that over 80 % of the studies relied on the ROI average-spectrum approach for information extraction, typically using conventional methods for multivariate model

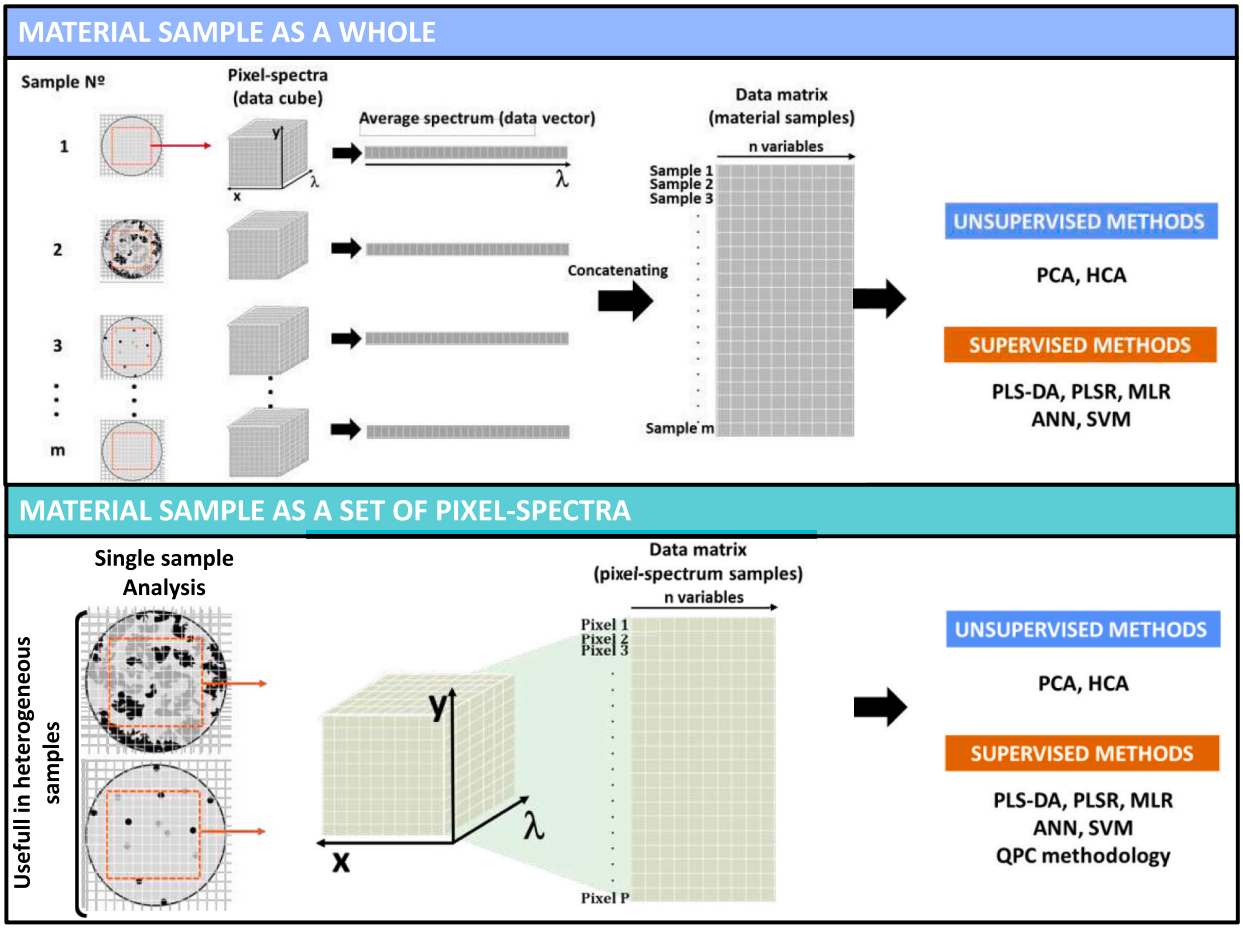

Fig. 5. Illustration of the main strategies for analyzing hyperspectral images: considering the material as a whole vs the material as a set of pixel spectra. PCA: principal component analysis; HCA: hierarchical clustering analysis; PLS-DA: partial least square-discriminant analysis; ANN: artificial neuronal networks; SVM: support vector machine; PLR: partial least square regression; MLR: multiple linear regression; QPC: quantification based on pixel counting by classification.

development with chemometric techniques. Only those studies that demonstrate a high degree of innovation in information extraction are examined in detail, with a focus on how these innovations contribute to improvements in the field.

4.1. *Adulteration detection*

Within animal-origin food products, beef and pork have been the primary focus of research. Both materials are inherently heterogeneous due to the presence of various tissues (e.g., muscle, fat) with different chemical compositions. As a result, most of these studies followed similar data analysis approaches. Initially, unsupervised machine learning methods were used to analyze natural groupings of ROI average spectra, with PCA being the most commonly applied tool. The material was first evaluated as a whole to determine whether the ROI average spectrum of adulterated samples could be distinguished from that of pure samples. In most studies, PCA was employed to identify the spectral regions with the highest variability between adulterated and pure samples. Following the unsupervised analysis, the same dataset (ROI average spectra) was used to develop classification models to differentiate between adulterated and pure materials. The most frequently applied chemometric tools were PLS-DA and SIMCA.

For example, Masithoh et al. [63] conducted a study to detect pork adulteration in lamb and beef meat. To achieve this, they employed the ROI average spectra of the analyzed materials, developing binary models aimed at classifying pure meat samples (lamb and beef) versus those adulterated with pork at different concentrations. PLSR was employed as a chemometric method, yielding promising results for the external validation set, with R^2 values of 0.7 and RMSE values between 3 % and 5 %. Additionally, a key innovation of the study was the detection of adulterated pixels within each sample by using the beta coefficients obtained from PLSR. This approach enabled the use of spectral information from pixels within the ROI to identify contaminated pixels and generate chemical concentration maps. These maps were created for each beef and lamb sample to evaluate the effectiveness of HSI in visualizing varying concentrations of pork adulteration. Achata et al. [65], in a similar way to Masithoh et al. [63], aimed to detect adulteration of beef with chicken, turkey, pork, and duck. To achieve this, they followed a similar strategy by first developing a classification model to distinguish between adulterated and non-adulterated samples, this time using PLS-DA, achieving over 90 % correct classification. Additionally, PLSR was used to quantify the percentage of adulterant. Subsequently, a chemical concentration map was generated to visualize the contaminated pixels. A notable aspect of this study is that, in addition to training and externally validating the models, the authors applied them in a second experiment. They used a new dataset to evaluate performance under real-world conditions, demonstrating their potential for routine analysis. In essence, the use of HSI for the detection of meat adulteration is recommended due to the heterogeneous nature of this material. Unlike point-based analytical techniques, HSI captures both spectral and spatial information from the entire sample, providing a more comprehensive and representative assessment. This is particularly relevant in meat fraud detection, where adulterants may not be homogeneously distributed within the sample. Furthermore, HSI offers significant advantages in terms of speed and simplicity compared to traditional analytical methods for these materials, such as DNA analysis.

Table 1
Hyperspectral imaging applications for detecting adulteration, contamination and non-conformity food fraud over the last five years: (A) animal-origin and (B) plant-based foodstuffs.

Material	Objective	Information mining	Spectral range (nm)	Machine learning	Food fraud	Ref.
(A) Animal-origin foodstuffs						
Alpaca	Detect, identify and quantify pork and beef adulteration in alpaca	• ROI average spectrum • ROI pixel-spectra	900–1700	PCA, SIMCA, PLS	Adulteration	[61]
Anchovies	Authentication of geographical origin and previous freeze process	• ROI average spectrum	400–1000 900–1700	PCA, SIMCA, PLS-DA	Non-conformity	[62]
Beef and lamb	Detect and quantify pork adulteration	• ROI average spectrum • ROI pixel-spectra	895–2504	PCA, PLSR	Adulteration	[63]
Beef	Detect, identify and quantify beef heart, liver or pork adulteration	• ROI average spectrum	900–1700	PCA, SIMCA, PLS-DA, CART, BP-ANN	Adulteration	[64]
	Detect, identify and quantify chicken, pork, turkey, lamb and duck adulteration	• ROI average spectrum	400–1000	PCA, PLSR, PLSDA	Adulteration	[65]
	Detect, identify and quantify chicken, pork, and duck adulteration	• ROI average spectrum	400–1000	PCA, PLS-DA, RF, kNN, SVM	Adulteration	[66]
	Detect and quantify soybean protein powder adulteration	• ROI pixel-spectra	380–1000	PCA, PLSR	Adulteration	[67]
	Detect chicken adulteration	• ROI average spectrum • ROI pixel-spectra	380–1000	PCR, PLSR	Adulteration	[68]
	Detect and quantify pork adulteration	• ROI average spectrum	890–2500	PLSR	Adulteration	[69]
Cheese	Detect and visualise bacterial contamination	• ROI average spectrum • ROI pixel-spectra	548–1701	PCA, PLS-DA	Contamination	[22]
Chicken	Detect and quantify of carrageenan adulteration	• ROI average spectrum	400–1000	PCA, PLSR	Adulteration	[70]
Honey	Detect sugar syrup adulteration	ROI average spectrum	864–1700	SCA, kNN, SVM	Adulteration	[71]
Lamb	Discrimination of pork adulterated lamb	• ROI average spectrum	1000–2500	CNN, SVM	Adulteration	[72]
		• ROI average spectrum	1000–2500	SVM, SVR	Adulteration	[73]
Mussels	Detect microplastics	• ROI pixel-spectra	1100–2500	N/A	Contamination	[74]
		• ROI pixel-spectra	1100–2500	N/A	Contamination	[75]
Pork	Detect and quantify offal adulteration	• ROI average spectrum • ROI pixel-spectra	400–1000	PCA, PLSR	Adulteration	[76]
	Detect and quantify porcine adulteration	• ROI average spectrum	400–1000	PCA, PLSR	Adulteration	[77]
	Detect and quantify bacterial contamination	• ROI average spectrum	400–1000	PLSR	Contamination	[78]
Salmon	Detect and quantify the proportion of Heilongjiang salmon used to adulterate Norwegian salmon	• ROI average spectrum	397–1003 935–1720	PCA, PLSR, CNN	Adulteration	[79]
Sea cucumber	Detect and identify sugar and salt adulteration	• ROI average spectrum	957–1679	SVM	Adulteration	[80]
(B) Plant-Based Foodstuffs						
Almonds	Detect bitter almonds presence	• ROI average spectrum	946–1648	PLS-DA	Non-conformity	[81]
	Detect, identify and quantify apricot and peanut adulteration	• ROI average spectrum	900–2494	PCA, SIMCA, PLSR	Adulteration	[82]
Black pepper	Detect, identify and quantify papaya seeds adulteration	• ROI average spectrum • ROI pixel-spectra	900–1710	PCA, PLSR, SIMCA	Adulteration	[83]
Chestnuts	Authentication of geographical origin	• ROI average spectrum	400–1000	PCA, PLS-DA, CNN	Non-conformity	[84]
Chickpea flour	Detect and quantify metanil yellow adulteration in chickpea flours	• ROI average spectrum	900–2500	PCA, PLSR, CNN	Adulteration	[20]
Cinnamon	Authenticate *Cinnamomum verum*	• ROI average spectrum • ROI pixel-spectra	953–1710	PCA, SVM, PLS-DA, SIMCA	Non-conformity	[85]

(*continued on next page*)

Table 1 (*continued*)

Material	Objective	Information mining	Spectral range (nm)	Machine learning	Food fraud	Ref.
Edible Oils	Detect adulterations of extra virgin olive oils with cheaper edible oils	• ROI average spectrum	900–1700	PCA, PLS-DA, SVM, RF, ANN	Adulteration	[57]
		• ROI average spectrum	900–1700	PCA, PLS-DA	Adulteration	[86]
		• ROI average spectrum	400–1000	SVM, LR, LDA, RF, DT, kNN, Naïve Bayes	Adulteration	[87]
Maize grain	Quantify mycotoxins levels	• ROI pixel-spectra	893–1730	PLSR	Contamination	[88]
		• ROI pixel-spectra	327–1093	SVR, CART, kNN	Contamination	[89]
	Detect, identify and quantify mycotoxins levels	• ROI pixel-spectra	400–1000	PCA, PLS-DA, PLSR	Contamination	[90]
Maize flower	Detect toxins contamination	• ROI pixel-spectra	900–1700	PLS-DA	Contamination	[91]
Mulberry	Detect and quantify fungicide contamination	• ROI average spectrum	270–850	PCA, PLSR	Contamination	[92]
Oregano	Detect, identify and quantify oregano adulteration with myrtle, olive and strawberry leaves.	• ROI average spectrum	980–1660	PCA, PLS-DA, SIMCA	Adulteration	[93]
Peanut	Detect mold contamination	• ROI average spectrum	930–2500	SVM	Contamination	[94]
Pomegranate molasses	Detect date syrup adulteration	• ROI average spectrum	700–1000	PCA, ABC	Adulteration	[95]
Pine nuts	Authentication of geographical origin	• ROI average spectrum • ROI pixel-spectra	940–1625	PCA, MCR, SIMCA	Non-conformity	[96]
Red chilli	Detect and identify wheat bran, rice bran, and saw dust adulteration	• ROI pixel-spectra	400–1000	PCA, SVM	Adulteration	[23]
Rice	Authentication of grain variety	• ROI average spectrum	400–1000	KNN, RF	Adulteration	[97]
	Detect fungal contamination	• ROI average spectrum	400–1000	PCA SVM	Contamination	[98]
	Detect paraffin contamination	• ROI average spectrum	250–2500	CNN, PLS-DA, SVM	Contamination	[99]
Saffron	Detect and quantify *Crocus sativus style* adulteration	• ROI average spectrum • ROI pixel-spectra	400–950	PCA, PLS-DA, SVM	Adulteration	[100]
	Detect, identify and quantify *Crocus sativus style*, safflower, madder, calendula and turmeric adulteration	• ROI average spectrum • ROI pixel-spectra	900–1710	PCA, HCA, PLS-DA, SIMCA	Adulteration	[101]
Spinach leaves	Detect fecal contamination	• ROI pixel-spectra	464–800 459–950	PLS-DA	Contamination	[102]
Sorghum	Detect adulterations with three varieties of sorghum	• ROI pixel-spectra	900–1700	PCA, PLS-DA	Adulteration	[103]
Tea	Detect adulterations with different teas	• ROI pixel-spectra	950–1760	PCA, SVM	Adulteration	[104]
Wheat grain	Detect and identify FHB-damaged	• ROI pixel-spectra	866–1701	CNN	Adulteration	[21]
Wheat flour	Detect, identify and quantify peanut, walnut and benzoyl peroxide adulteration	• ROI average spectrum	380–1030	SACNN	Adulteration	[105]
Wholemeal flour	Quantify wholemeal flour in bread	• ROI average spectrum • QPC	400–1000	PCA, SVM, PLS-DA	Non-conformity	[24]
Wolfberry	Detect sulphur particles adulteration	• ROI average spectrum	900–1700	LDA, KNN, PLSR, SVM	Adulteration	[106]
Yam	Authentication of geographical origin	• ROI average spectrum	400–1000	PLS-DA, SVM, RF	Non-conformity	[107]

ABC: artificial beer colony; BP-ANN: back propagation-artificial neuronal networks; CART: classification and regression tree; CNN: convolutional neuronal networks; DT: Decision tree; EDM: Euclidean distance measure; kNN: K-Nearest neighbours; LR: Logistic regression; SAM: spectral angel measure; SCM: spectral correlation measure; PCA: principal component analysis; PLS: partial least square; PLS-DA: partial least square discriminant analysis; PLSR: partial least square regression; QPC: quantification based on pixel counting by classification; SACNN: symmetric all convolutional neuronal networks; SDA: stepwise discriminant analysis; SVM: support vector machine; SIMCA: soft independent modelling of class analogies; SPA-LDA: Successive projections coupled with linear discriminant analysis; SVR: support vector regression; N/A: Not applicable.

Regarding other solid-state food products, studies focused on the authentication of flours are particularly noteworthy, as ROI pixel spectra are frequently used to develop classification models. Although flour may seem homogeneous, it has inherent heterogeneity due to factors such as particle size or the blending of flours from different origins or qualities, which complicates its precise characterization using conventional point-based analytical methods. HSI overcomes these limitations, as demonstrated by several studies. For instance, Zhen et al. [105] used neural networks to detect wheat flour adulteration with peanut, walnut, or benzoyl peroxide, performing variable selection prior to model development and achieving accuracy and area under the curve (AUC) values above 90 %.

Finally, it is important to consider the analysis of liquid foods, such as olive oil. The application of HSI to these samples remains a topic of

debate. This happens because the inherent homogeneity of liquid matrices, which lack spatial heterogeneity, often makes more cost-effective techniques—such as FTIR, NIR, or Raman spectroscopy—sufficient, potentially rendering HSI unnecessary. In this context, Malavi et al. [57] conducted a comparative study employing various analytical techniques, including FTIR, GC–MS, UV–Vis, and HSI, to detect the adulteration of olive oil with other edible vegetable oils. Their results showed that these techniques produced similar outcomes, indicating that HSI has potential for such applications. However, the complexity of data processing associated with HSI is considerably higher compared to techniques like UV–Vis or FTIR, suggesting that HSI may not be the most suitable choice. Similarly, Aqeel et al. [86] applied HSI for the same purpose as Malavi et al. and concluded that HSI, in combination with machine learning methods, yielded good results in detecting adulteration with other vegetable oils, such as soybean or sesame oil. Their models were constructed using ROI average spectrum in the NIR range, which is consistent with the extensive literature supporting the use of NIR spectroscopy for olive oil authentication. Therefore, the added value of HSI in this context may be limited, like some authors have demonstrated (see Tazilli et al. [38]). These authors argue that, although HSI provides more extensive spatial information, which should theoretically offer an advantage, there are situations where it is not essential. In such cases, NIR spectrophotometer probes, for instance, can effectively address the issue.

4.2. Contamination detection

In the context of contamination detection, the most widely used approach for model construction is the ROI pixel spectra. It is appropriate because contamination detection requires pixel-by-pixel analysis to accurately locate and characterize the contaminant. For example, several studies have used ROI pixel-spectra to detect mycotoxin contamination in grains. Borrás-Vallverdú et al. [88] used NIR-HSI combined with PLS to detect and quantify various mycotoxins (DON, FB1, FB2) in maize kernels. Additionally, the authors proposed a classification based on mycotoxin concentration levels, which yielded better results than direct quantification, achieving sensitivity, specificity, and accuracy values ranging from 70 % to 90 %. Wang et al. [89] conducted a similar study, focusing exclusively on the detection and quantification of aflatoxin B1 using fluorescence HSI. These authors further reported that nonlinear learning methods are more suitable for such studies, as classification models tend to outperform linear approaches. They concluded that applying a boosting-stacking method can significantly enhance regression performance.

Other studies have focused on detecting microplastic contamination. In this regard, Piarulli et al. [74,75] published two studies aimed at detecting different plastics in mussels (low-density polyethylene (LDPE) in one study, and polypropylene (PP), polystyrene (PS), and polyamide (PA) in the other). In both studies, NIR-HSI was applied, first separating the soft tissue from the shell and conducting pre-treatment of the sample before analysis. Once the image was captured, a chemical map based on the ROI pixel spectra was generated using a normalized difference image (NDI). To reduce the data and simplify the interpretation of the results, each pixel's NDI value was represented by a color scale ranging from red (highest value) to blue (lowest value). This created an RGB chemical map indicating the presence of microplastics. Specifically, pixels corresponding to microplastic particles exhibited the highest NDI ratio, appearing red on the map. Using this information extraction approach, the authors developed a new analytical methodology for detecting these target microplastics. They concluded that, although the spatial resolution of the NIR-HSI system is lower than that of other microscale spectroscopic techniques—which can detect microplastics as small as 11 μm—it still presents clear advantages. The rapid and highly automatable analytical workflow of NIR-HSI offers an efficient and cost-effective method for examining large numbers of environmental samples. They can include complex, heterogeneous matrices, directly on filters and without the need for extensive sample preparation.

4.3. Non-compliance detection

In studies focused on detecting food non-conformities, 90 % of studies use ROI average spectrum information to build multivariate models, predominantly aimed at authenticating the geographic origin. Esplandiú et al. [62], Li et al. [84], and Zhang et al. [107] developed models aiming to authenticate the geographical origin of anchovies, chestnuts, and yam. In the anchovy study, the authors employed PLS-DA, and the results revealed that models based on the VIS-NIR spectral range outperformed those using only the NIR region. In the chestnut study, PLS-DA and deep learning methods such as one-dimensional convolutional neural network (1D-CNN) were tested. PLS-DA and 1D-CNN models achieved prediction accuracies above 95 %, and both sensitivities and specificities for PLS-DA and 1D-CNN models exceeded 90 % for the samples from each geographical origin. Therefore, from these results and considering the complexity involved in developing neural network-based models, PLS-DA stands out as a suitable method for addressing this type of problem. In the yam study, PLS-DA, SVM and Random Forest (RF) were selected as machine learning methods to build the different origin authentication models. For this purpose, not only was the ROI average spectrum used, but models were also developed by selecting specific wavelengths of interest using the successive projections algorithm (SPA). Accuracy values of 100 % were achieved for the training set, and 98.40 % for the external validation set.

Other studies have combined both approaches (ROI average spectrum and ROI pixel spectra) to examine non-conformities. For example, Medina et al. [24] developed models aimed at classifying the type of flour used in bread production, distinguishing between whole wheat and white flour, and quantifying the proportion of whole wheat flour present. Notably, this study introduced an innovative combination of ROI average spectrum and ROI pixel spectra with machine learning methods such as SVM, achieving precision values over 80 %. Ríos-Reina et al. [96] studied the feasibility of the HSI application to authenticate the geographical origin of pine nuts. For this, PCA and MCR were applied to the ROI average spectrum of each material. Subsequently, ROI pixel spectra were used to develop a classification model capable of distinguishing materials from different geographical origins.

5. Challenges and limitations of HSI in the food industry

Translating the potential of NIR-HSI into robust, routine use in industrial or regulatory contexts presents several challenges. Understanding the specific limitations of HSI within the food domain is critical to developing practical, scalable, and scientifically sound solutions. Some factors that need to be considered are:

(i) High data dimensionality vs. real-time requirements. HSI generates massive datasets with hundreds of spectral bands and up to thousands or millions of pixels. In food industry settings, where fast decision-making and high-throughput inspection are essential (e.g., conveyor belt sorting, online quality control), this becomes a significant bottleneck. Although data reduction techniques, such as variable selection, PCA, or band selection can help, achieving real-time or near-real-time performance remains a technological and computational challenge.

(ii) Variability in food matrices. Food products are inherently variable and often complex in composition and structure. This includes moisture gradients, non-uniform textures, irregular shapes, and inhomogeneities, all of which can influence the spectral signal. Unlike well-controlled lab samples, real-world food items often introduce spectral variability which complicates calibration and interpretation. Accounting for this natural variability is critical for building reliable models that can generalize across batches, seasons, or processing lines.

(iii) Influence of surface properties and geometry. The quality of HSI data can be significantly influenced by surface conditions, such as glossiness, roughness, or irregular contours, which affect light scattering and reflectance. In solid or semi-solid foods (e.g., cheese, bakery products, meats), surface geometry can cause shadowing or variable illumination, introducing artifacts into the spectra. This becomes especially problematic when using reflectance-mode imaging in industrial environments, where maintaining consistent lighting can be challenging.

(iv) Spatial resolution vs. particle size. When targeting specific features such as contaminants, bruises, fungal growth, or foreign particles, the spatial resolution of the system must match or exceed the size of these features. Otherwise, mixed pixels may obscure their detection. This constraint is particularly relevant in the production of flour, spices, cereals, and powders, where small particles or defects must be accurately detected and resolved for safety and quality control purposes.

(v) Calibration and ground truth building challenges. Supervised analysis in food HSI requires reliable reference values for both qualitative and quantitative tasks. Acquiring these reference values is often labour-intensive and destructive, which limits the number of labelled samples and complicates model development. Inconsistent or poorly aligned ground truth data is one of the major obstacles to robust model training and validation in food applications.

(vi) Limited transferability and standardization. Models developed on a specific HSI system or under tightly controlled lab conditions often struggle when transferred to different instruments, processing lines, or lighting setups. This lack of standardization in both the hardware and analysis protocols hampers scalability and adoption in industrial environments. In the absence of universal calibration procedures or spectral libraries, each application often requires its custom-built model.

(vii) Regulatory and practical barriers. Even when HSI is scientifically validated, deploying it at scale in the food industry faces practical constraints, including high system costs, integration with existing production lines, the need for technical expertise, and the regulatory approval of HSI-based methods. Furthermore, for critical safety or quality decisions, food companies and regulatory agencies often favour methods that are interpretable, traceable, and well-validated.

6. Conclusions and outlook

Hyperspectral imaging has emerged as a transformative analytical tool for assessing food quality, safety, and authenticity. Its unique combination of spatial and spectral resolution allows for non-destructive, rapid, and environmentally friendly analysis of diverse food matrices, whether solid or liquid, homogeneous or heterogeneous. Over the past decade, advances in sensor design, combined with developments in both classical chemometric modelling and modern machine learning techniques, have significantly expanded the scope of HSI applications across the food sector.

HSI has demonstrated its value in addressing critical food industry concerns, including adulteration, contamination, and non-conformity fraud. Its ability to extract both qualitative and quantitative information, ranging from compositional analysis to spatial distribution and physical attributes, positions it as a comprehensive platform for quality assurance and fraud detection. However, despite its analytical strengths, several practical and technical challenges continue to limit its broader industrial implementation.

Key limitations include high capture system costs, substantial computational demands, and the lack of standardized acquisition protocols and data processing workflows. These factors hinder reproducibility, model transferability, and inter-laboratory comparability. Establishing industry-wide standards for spectral data formats, preprocessing routines, and validation procedures is essential to enable scalable deployment and regulatory acceptance.

Machine learning and deep learning algorithms offer promising pathways to automate spectral interpretation and enhance classification accuracy. However, their adoption must be balanced with concerns over model transparency and interpretability, especially in regulated environments where decision traceability is paramount. The role of classical chemometrics remains highly relevant in this context, offering more interpretable models that align well with industrial and regulatory expectations.

Further progress in sensor miniaturization and the development of cost-effective materials are expected to facilitate the production of portable and affordable HSI devices. These innovations will help integrate HSI into routine inspection settings, including in-field, at-line, and online environments. At the same time, advances in understanding the interaction of radiation with complex food matrices will improve the analysis of internal features, making the technique even more powerful for non-invasive characterization.

Finally, HSI holds untapped potential in supporting sustainability goals, such as reducing food waste through freshness assessment and spoilage prediction. To fully realize this potential, continued interdisciplinary collaboration among researchers, engineers, food scientists, and industry stakeholders is essential. By addressing its current limitations and advancing both technology and methodology, HSI is poised to become not only a research innovation but also a standard tool for ensuring food quality and safety across global supply chains.

CRediT authorship contribution statement

Miriam Medina–García: Writing – original draft, Investigation, Conceptualization. **José M. Amigo:** Writing – review & editing, Validation, Methodology, Investigation. **Miguel A. Martínez-Domingo:** Writing – review & editing, Methodology, Investigation, Conceptualization. **Eva M. Valero:** Writing – review & editing, Methodology, Investigation, Formal analysis. **Ana M. Jiménez–Carvelo:** Writing – review & editing, Supervision, Resources, Project administration, Methodology, Investigation, Funding acquisition, Conceptualization.

Funding

Grant (RYC2021-031993-I) funded by MCIU/AEI/501100011033 and "European Union NextGenerationEU/PRTR".

Declaration of competing interest

The authors declare that they have no known competing financial interests or personal relationships that could have appeared to influence the work reported in this paper.

Acknowledgements

AMJC acknowledges the Grant (RYC2021-031993-I) funded by MICIU/AEI/501100011033 and "European Union NextGeneration EU/PRTR". Funding for open access charge: Universidad de Granada / CBUA.

Data availability

No data was used for the research described in the article.

References

[1] FAO (Food and Agrlicultural Organitacion). Assuring food safety and quality. Guidelines for strengthening national food control systems. In: FAO nutrition paper, 76. https://openknowledge.fao.org/server/api/core/bitstreams/695e85e5-acdc-441a-a969-d36cb76c1c8e/content. Accessed 2 Sep 2024.

[2] Rhodehamel EJ, Overview of biological, chemical, and physical hazards. In: Pierson MD, Corlett D.A, editors. HACCP Principles and applications. London: Champman & Hall; 1992. pp.8-28. doi: 10.1007/978-1-4684-8818-0_3.

[3] S. Togan, Food safety: a developing country perspective, Cent Eur Econ J. 11 (2024) 54–66, https://doi.org/10.2478/ceej-2024-0006.

[4] Paparella, A, Allergenic hazards. In: Abu Al-Rub F, Shibhab P, Abu Al-Rub S, Pittia P, Paparella A, editors. Food safety hazards. Lisle: GAVIN eBooks; 2020. pp. 39-49. doi: 10.29011/978-1-951814-03-8-005.

[5] W.H. Oldewage-Theron, A.A. Egal, Food quality and food safety, in: N.J. Temple, N. Steyn (Eds.), Community Nutrition for Developing Countries, Athabasca University Press and UNISA Press, Edmonton, 2016, pp. 430–449, https://doi.org/10.15215/aupress/9781927356111.01.

[6] S.M. Van Ruth, W. Huisman, P.A. Luning, Food fraud vulnerability and its key factors, Trends Food Sci Technol. 67 (2017) 70–75, https://doi.org/10.1016/j.tifs.2017.06.017.

[7] Commission Regulation (EU) No 20219/1715. 2019. Laying down rules for the functioning of the information management system for official controls and its system components ('the IMSOC Regulation').

[8] European Commission. 2024. Monthly summary of articles on food fraud an adulteration. https://knowledge4policy.ec.europa.eu/file/food-fraud-summary-june-2024_en. Accessed 2 Sep 2024.

[9] Ducauze CJ. Fraudes alimentarios: legislación y metodología analítica. 1st ed. Acribia; 2006.

[10] P. Viscinao, M. Schirone, Food Frauds: Global incidents and misleading situations, Trends Food Sci Technol. 114 (2021) 424–442, https://doi.org/10.1016/j.tifs.2021.06.010.

[11] B. Modi, H. Timilsina, S. Bhandari, A. Achhami, S. Pakka, P. Shrestha, N. Parajuli, Current trends of food analysis, safety, and packaging. Int, J Food Sci. 924667 (2021), https://doi.org/10.1155/2021/9924667.

[12] S. Medina, R. Perestrelo, P. Silva, J.A.M. Pereira, J.S. Câmara, Current trends and recent advances on food authenticity technologies and chemometric approaches, Trends Food Sci Technol. 85 (2019) 163–176, https://doi.org/10.1016/j.tifs.2019.01.017.

[13] A. Khan, M.T. Munir, W. Yu, B.R. Young, A review towards hyperspectral imaging for real-time quality control of food products with an illustrative case study of milk powder production, Food Bioproc Tech. 13 (2020) 739–752, https://doi.org/10.1007/s11947-020-02433-w.

[14] A.F. Goetz, G. Vane, J.E. Solomon, B.N. Rock, Imaging spectroscopy for earth remote sensing, Science 228 (1985) 1147–1153, https://doi.org/10.1126/science.228.4704.1147.

[15] Y.H. El-Sharkawy, Advancements in non-invasive hyperspectral imaging: Mapping blood oxygen levels and vascular health for clinical and research applications, Vasc Pharmacol. 107380 (2024), https://doi.org/10.1016/j.vph.2024.107380.

[16] H.T. Temiz, B. Ulaş, A review of recent studies employing hyperspectral imaging for the determination of food adulteration, Photochem. 1 (2021) 125–146, https://doi.org/10.3390/photochem1020008.

[17] J.M. Amigo, Hyperspectral imaging, 1st ed., Elsevier, Amsterdam, 2019.

[18] J. Ma, D.W. Sun, H. Pu, J.H. Cheng, Q. Wei, Advanced Techniques for hyperspectral imaging in the food industry: Principles and recent applications, Annu Rev Food Sci Technol. 10 (2019) 197–220, https://doi.org/10.1146/annurev-food-032818-121155.

[19] G.E.L. Masry, D.W. Sun, Principles of hyperspectral imaging technology, in: D. W. Sun (Ed.), Hyperspectral Imaging for Food Quality Analysis and Control, Academic Press, London, 2010, pp. 3–43.

[20] D. Saha, T. Senthilkumar, C.B. Singh, A. Manickavasagan, Quantitative detection of metanil yellow adulteration in chickpea flour using line-scan near-infrared hyperspectral imaging with partial least square regression and one-dimensional convolutional neural network, J Food Compos Anal. 120 (2023) 105290, https://doi.org/10.1016/j.jfca.2023.105290.

[21] J. Zhu, Z. Rao, H. Ji, Fast and simultaneous detection of wheat kernel adulteration using hyperspectral imaging technology and deep convolutional neural network, J Food Saf. 44 (2024) e13133, https://doi.org/10.1111/jfs.13133.

[22] M.M. Reis, Y. Dixit, A. Carr, C. Tu, F. Palevich, T. Gupta, M.G. Reis, Hyperspectral imaging through vacuum packaging for monitoring cheese biochemical transformation caused by Clostridium metabolism, Food Res Int. 169 (2023) 112866, https://doi.org/10.1016/j.foodres.2023.112866.

[23] M.H. Khan, Z. Saleem, M. Ahmad, A. Sohaib, H. Ayaz, M. Mazzara, R.A. Raza, Hyperspectral imaging-based unsupervised adulterated red chili content transformation for classification: Identification of red chili adulterants, Neural Comput Appl. 33 (2021) 14507–14521, https://doi.org/10.1007/s00521-021-06094-4.

[24] M. Medina-García, E.A. Roca-Nasser, M.A. Martínez-Domingo, E.M. Valero, A. Arroyo-Cerezo, L. Cuadros-Rodríguez, A.M. Jiménez-Carvelo, Towards the establishment of a green and sustainable analytical methodology for hyperspectral imaging-based authentication of wholemeal bread, Food Control 166 (2024) 110715, https://doi.org/10.1016/j.foodcont.2024.110715.

[25] C. Wang, B. Liu, L. Liu, Y. Zhu, J. Hou, P. Liu, X. Li, A review of deep learning used in the hyperspectral image analysis for agriculture, Artif Intell Rev. 54 (2021) 5205–5253, https://doi.org/10.1007/s10462-021-10018-y.

[26] N. Gul, K. Muzaffar, S.Z.A. Shah, A. Assad, H.A. Makroo, B.N. Dar, Deep learning hyperspectral imaging: a rapid and reliable alternative to conventional techniques in the testing of food quality and safety, Qual Assur Saf Crop. 16 (2024) 78–97, https://doi.org/10.15586/qas.v16i1.1392.

[27] A.I. Durojaiye, S.T. Olorunsogo, B.A. Adejumo, A. Babawuya, I.I. Muhamad, Deep learning techniques for the exploration of hyperspectral imagery potentials in food and agricultural products, Food Hum. 3 (2024) 100365, https://doi.org/10.1016/j.foohum.2024.100365.

[28] M. Nikzadfar, M. Rashvand, H. Zhang, A. Shenfield, F. Genovese, G. Altieri, A. Matera, I. Tornese, S. Laveglia, G. Paterna, C. Lovallo, O. Mammadov, B. Aykanat, G.C. Di Renzo, Appl Sci. 14 (2024) 9821, https://doi.org/10.3390/app14219821.

[29] D. Saha, A. Manickavasagan, Machine learning techniques for analysis of hyperspectral images to determine quality of food products: A review, Curr Res Food Sci. 4 (2021) 28–44, https://doi.org/10.1016/j.crfs.2021.01.002.

[30] Z. Kang, Y. Zhao, L. Chen, Y. Guo, Q. Mu, S. Wang, Advances in machine learning and hyperspectral imaging in the food supply chain, Food Eng Rev. 14 (2022) 596–616, https://doi.org/10.1007/s12393-022-09322-2.

[31] Chaudhry MMA, Babellahi F, Amodio ML, Colelli G, Sahar A. Image analysis. In. Iqbal Khan MK, editor. Advances in Noninvasive Food Analysis. Boca Raton: CRC Press; 2019.pp. 199-227.

[32] NBasantia NC, Nollet LM, Kamruzzaman M. Hyperspectral imaging analysis and applications for food quality. 1st ed. Boca Raton: CRC Press; 2019. doi: 10.1201/9781315209203.

[33] Y. Wang, X. Ou, H.J. He, M. Kamruzzaman, Advancements, limitations and challenges in hyperspectral imaging for comprehensive assessment of wheat quality: An up-to-date review, Food Chem x. 21 (2024) 101235, https://doi.org/10.1016/j.fochx.2024.101235.

[34] C.M. Peraza-Alemán, A. López-Maestresalas, C. Jarén, N. Rubio-Padilla, S. A. Arazuri, Systematized review on the applications of hyperspectral imaging for quality control of potatoes, Potato Res. 67 (2024) 1539–1561, https://doi.org/10.1007/s11540-024-09702-7.

[35] L. Li, X. Jia, K. Fan, Recent advance in nondestructive imaging technology for detecting quality of fruits and vegetables: A review, Crit Rev Food Sci Nutr. (2024), https://doi.org/10.1080/10408398.2024.2404639.

[36] A. Ismail, D.G. Yim, G. Kim, C. Jo, Hyperspectral imaging coupled with multivariate analyses for efficient prediction of chemical, biological and physical properties of seafood products, Food Eng Rev. 15 (2023) 41–55, https://doi.org/10.1007/s12393-022-09327-x.

[37] R.T. Matenda, D. Rip, J. Marais, P.J. Williams, Exploring the potential of hyperspectral imaging for microbial assessment of meat: A review, Spectrochim Acta A Mol Biomol Spectrosc. 315 (2024) 124261, https://doi.org/10.1016/j.saa.2024.124261.

[38] D. Tazilli, M. Cocchi, J.M. Amigo, A. D'Alessandro, L. Strani, Does hyperspectral always matter? A critical assessment of near infrared versus hyperspectral near infrared in the study of heterogeneous samples, Curr Res Food Sci. 9 (2024) 100813, https://doi.org/10.1016/j.crfs.2024.100813.

[39] Vane G. Airborne Visible/Infrared Imaging Spectrometer (AVIRIS): A description of the sensor, ground data processing facility, laboratory calibration, and first results. NASA Technical Reports Server. 1987. https://ntrs.nasa.gov/citations/19880004943. Accessed 11 Jan 2025.

[40] G. Kortüm, Reflectance spectroscopy: principles, methods, applications, 1st ed., Springer, Berlin, 1969.

[41] P. Hemrattrakun, K. Nakano, D. Boonyakiat, S. Ohashi, P. Maniwara, P. Theanjumpol, P. Seehanam, Comparison of reflectance and interactance modes of visible and near-infrared spectroscopy for predicting persimmon fruit quality. Food Anal, Methods 14 (2021) 117–126, https://doi.org/10.1007/s12161-020-01853-w.

[42] H.W. Siesler, Y. Ozaki, S. Kawata, H.M. Heise, Instrumentation for near-infrared spectroscopy, in: H.W. Siesler, Y. Ozaki, S. Kawata, H.M. Heise (Eds.), Near Infrared Spectroscopy, Principles, Instruments, Applications, Wiley, Weinheim, 2008, pp. 43–74, https://doi.org/10.1002/9783527612666.ch03.

[43] L.W. Sun, X. Ye, W. Fang, Z.L. He, X.L. Yi, Y.P. Wang, Radiometric calibration of hyper-spectral imaging spectrometer based on optimizing multi-spectral band selection, Optoelectron Lett. 13 (2017) 405–408, https://doi.org/10.1007/s11801-017-7174-7.

[44] S. Chatti, L. Laperrière, G. Reinhart, T. Tolio, CIRP: The International academy for production engineering. Encyclopedia of production engineering, 2nd ed., Springer, Berlin, 2019.

[45] S.T. McHugh, Understanding Photography: Master Your Digital Camera and Capture That Perfect Photo, 1st ed., No Starch Press, San Francisco, 2018.

[46] S.C. Yoon, B. Park, Hyperspectral image processing methods, in: P. Bosoon, L. Renfu (Eds.), Hyperspectral Imaging Technology in Food and Agriculture, Springer, London, 2015, pp. 81–101, https://doi.org/10.1007/978-1-4939-2836-1.

[47] A. Bhargava, A. Sachdeva, K. Sharma, M.H. Alsharif, P. Uthansakul, M. Uthansakul, Hyperspectral Imaging and its applications: A Review, Heliyon. 10 (2024) e33208, https://doi.org/10.1016/j.heliyon.2024.e33208.

[48] N. Hagen, M.W. Kudenov, Review of snapshot spectral imaging technologies, Opt Eng. 52 (2013) 090901, https://doi.org/10.1117/1.OE.52.9.090901.

[49] M.A. Martínez-Domingo, E.M. Valero, J. Hernández-Andrés, S. Tominaga, T. Horiuchi, K. Hirai, Image processing pipeline for segmentation and material classification based on multispectral high dynamic range polarimetric images, Opt Express. 25 (2017) 30073–30090, https://doi.org/10.1364/OE.25.030073.

[50] E.M. Valero, M.A. Martínez, E. Kirchner, I. van der Lans, M. García-Fernández, T. Eckhard, R. Huertas, Framework proposal for high-resolution spectral image acquisition of effect-coatings, Measurement 145 (2019) 379–390, https://doi.org/10.1016/j.measurement.2019.05.024.

[51] C.M. Sun, Y. Yuan, Q.B. Lv, Spectral image reconstruction of coded aperture spectral imaging system based on compressed sensing, AOPC. 12558 (2023) 131–136, https://doi.org/10.1117/12.2652057.
[52] K.A. Sneha, Hyperspectral imaging and target detection algorithms: a review, Multimed Tools Appl. 81 (2022) 44141–44206, https://doi.org/10.1007/s11042-022-13235-x.
[53] J. Wieme, K. Mollazade, I. Malounas, M. Zude-Sasse, M. Zhao, A. Gowen, J. Van Beek, Application of hyperspectral imaging systems and artificial intelligence for quality assessment of fruit, vegetables and mushrooms: A review, Biosyst Eng. 222 (2022) 156–176, https://doi.org/10.1016/j.biosystemseng.2022.07.013.
[54] Y. Xu, J. Zhang, Y. Wang, Recent trends of multi-source and non-destructive information for quality authentication of herbs and spices, Food Chem. 398 (2023) 133939, https://doi.org/10.1016/j.foodchem.2022.133939.
[55] D. Patel, S. Bhise, S.S. Kapdi, T. Bhatt, Non-destructive hyperspectral imaging technology to assess the quality and safety of food: a review, Food Prod Process Nu. 6 (2024) 69, https://doi.org/10.1186/s43014-024-00246-4.
[56] K.W. Whitten, General Chemistry, 7th ed., Brooks/Cole Publishing Company, Pacific Grove, 2004.
[57] D. Malavi, A. Nikkhah, K. Raes, S. Van Haute, Hyperspectral imaging and chemometrics for authentication of extra virgin olive oil: A comparative approach with FTIR, UV-VIS, Raman, and GC-MS, Foods. 12 (2023) 429, https://doi.org/10.3390/foods12030429.
[58] J.M. Amigo, I. Martí, A. Gowen, Hyperspectral imaging and chemometrics: a perfect combination for the analysis of food structure, composition and quality. Data handling in science and technology, Elsevier (2013) 343–370, https://doi.org/10.1016/B978-0-444-59528-7.00009-0.
[59] L. Cuadros-Rodríguez, E. Pérez-Castaño, C. Ruiz-Samblás, Quality performance metrics in multivariate classification methods for qualitative analysis, Trends Anal Chem. 80 (2017) 612–624, https://doi.org/10.1016/j.trac.2016.04.021.
[60] Astm, E2617-17, Standard practice for validation of empirically derived multivariate calibrations, ASTM International, West Conshohocken, PA (2017), https://doi.org/10.1520/E2617-17.
[61] J.P. Cruz-Tirado, M.S. dos Santos Vieira, O.O.V. Correa, D.R. Delgado, J. M. Angulo-Tisoc, D.F. Barbin, R. Siche, Detection of adulteration of Alpaca (Vicugna pacos) meat using a portable NIR spectrometer and NIR-hyperspectral imaging, J Food Compos Anal. 126 (2024) 105901, https://doi.org/10.1016/j.jfca.2023.105901.
[62] P.L. Esplandiú, J.J. Marín-Méndez, M. Alonso-Santamaría, B. Remírez-Moreno, M.J. Sáiz-Abajo, Fraud detection in the fishing sector using hyperspectral imaging, J near Infrared Spectrosc. 32 (2024) 69–80, https://doi.org/10.1177/09670335241258667.
[63] R.E. Masithoh, M.F.R. Pahlawan, J. Kim, M.A.A. Arief, H. Kurniawan, R.A. P. Hernanda, B.K. Cho, Shortwave infrared hyperspectral imaging for the determination of pork adulteration in minced beef and lamb, Food Control 166 (2024) 110736, https://doi.org/10.1016/j.foodcont.2024.110736.
[64] W. Jia, A. Ferragina, R. Hamill, A. Koidis, Modelling and numerical methods for identifying low-level adulteration in ground beef using near-infrared hyperspectral imaging (NIR-HSI), Talanta 276 (2024) 126199, https://doi.org/10.1016/j.talanta.2024.126199.
[65] E.M. Achata, M.A. Mousa, A.D. Al-Qurashi, O.H. Ibrahim, K.A. Abo-Elyousr, A.M. A. Aal, M. Kamruzzaman, Multivariate optimization of hyperspectral imaging for adulteration detection of ground beef: Towards the development of generic algorithms to predict adulterated ground beef and for digital sorting, Food Control 153 (2023) 109907, https://doi.org/10.1016/j.foodcont.2023.109907.
[66] H. Jiang, W. Yuan, Y. Ru, Q. Chen, J. Wang, H. Zhou, Feasibility of identifying the authenticity of fresh and cooked mutton kebabs using visible and near-infrared hyperspectral imaging, Spectrochim Acta A Mol Biomol Spectrosc. 182 (2022) 121689, https://doi.org/10.1016/j.saa.2022.121689.
[67] H. Jiang, X. Jiang, Y. Ru, Q. Chen, J. Wang, L. Xu, H. Zhou, Detection and visualization of soybean protein powder in ground beef using visible and near-infrared hyperspectral imaging, Infrared Phys Technol. 127 (2022) 104401, https://doi.org/10.1016/j.infrared.2022.104401.
[68] Z. Zhao, H. Yu, S. Zhang, Y. Du, Z. Sheng, Y. Chu, L. Deng, Visualization accuracy improvement of spectral quantitative analysis for meat adulteration using Gaussian distribution of regression coefficients in hyperspectral imaging, Optik 212 (2020) 164737, https://doi.org/10.1016/j.ijleo.2020.164737.
[69] R.E. Masithoh, R.A.P. Hernanda, M.F.R. Pahlawan, J. Kim, H.Z. Amanah, B. K. Cho, Shortwave near Infrared–hyperspectral imaging spectra to detect pork adulteration in beef using partial least square regression coupled with vip wavelength selections method, Optics. 6 (2025) 1, https://doi.org/10.3390/opt6010001.
[70] Y. Zhang, H. Jiang, W. Wang, Feasibility of the detection of carrageenan adulteration in chicken meat using visible/near-infrared (VIS/NIR) hyperspectral imaging, Appl Sci 9 (2019) 3926, https://doi.org/10.3390/app9183926.
[71] D.B. Siano, W. Abdullakasim, A. Terdwongworakul, K. Phuangsombut, Improving the performance of the model developed from the classification of adulterated honey with different botanical origins based on near-Infrared hyperspectral imaging system and supervised classification algorithms, Infrared Phys. Technol. 131 (2023) 104692, https://doi.org/10.1016/j.infrared.2023.104692.
[72] Z. Huang, B. Li, S. Wang, R. Zhu, X. Cui, X. Yao, Robust and accurate classification of mutton adulteration under food additives effect based on multi-part depth fusion features and optimized support vector machine, Food Anal Methods. 16 (2023) 933–946, https://doi.org/10.1007/s12161-023-02459-8.
[73] B. Fan, R. Zhu, D. He, S. Wang, X. Cui, X. Yao, Evaluation of mutton adulteration under the effect of mutton flavour essence using hyperspectral imaging combined with machine learning and sparrow search algorithm, Foods. 11 (2022) 2278, https://doi.org/10.3390/foods11152278.
[74] S. Piarulli, C. Malegori, F. Grasselli, L. Airoldi, S. Prati, R. Mazzeo, P. Oliveri, An effective strategy for the monitoring of microplastics in complex aquatic matrices: Exploiting the potential of near infrared hyperspectral imaging (NIR-HSI), Chemosphere 286 (2022) 31861, https://doi.org/10.1016/j.chemosphere.2021.131861.
[75] S. Piarulli, G. Sciutto, P. Oliveri, C. Malegori, S. Prati, R. Mazzeo, L. Airoldi, Rapid and direct detection of small microplastics in aquatic samples by a new near infrared hyperspectral imaging (NIR-HSI) method, Chemosphere 260 (2020) 127655, https://doi.org/10.1016/j.chemosphere.2020.127655.
[76] H. Jiang, Y. Ru, Q. Chen, J. Wang, L. Xu, Near-infrared hyperspectral imaging for detection and visualization of offal adulteration in ground pork, Spectrochim Acta A Mol Biomol Spectrosc. 249 (2021) 119307, https://doi.org/10.1016/j.saa.2020.119307.
[77] H. Jiang, F. Cheng, M. Shi, Rapid identification and visualization of jowl meat adulteration in pork using hyperspectral imaging, Foods. 9 (2022) 154, https://doi.org/10.3390/foods9020154.
[78] E. Bonah, X. Huang, J.H. Aheto, R. Yi, S. Yu, H. Tu, Comparison of variable selection algorithms on vis-NIR hyperspectral imaging spectra for quantitative monitoring and visualization of bacterial foodborne pathogens in fresh pork muscles, Infrared Phys Technol. 107 (2020) 103327, https://doi.org/10.1016/j.infrared.2020.103327.
[79] P. Li, S. Tang, S. Chen, X. Tian, N. Zhong, Hyperspectral imaging combined with convolutional neural network for accurately detecting adulteration in Atlantic salmon, Food Control 147 (2023) 109573, https://doi.org/10.1016/j.foodcont.2022.109573.
[80] X. Zhang, J. Sun, P. Li, F. Zeng, H. Wang, Hyperspectral detection of salted sea cucumber adulteration using different spectral preprocessing techniques and SVM method, LWT-Food Sci Technol 152 (2021) 112295, https://doi.org/10.1016/j.lwt.2021.112295.
[81] I. Torres-Rodríguez, M.T. Sánchez, J.A. Entrenas, M. Vega-Castellote, A. Garrido-Varo, D. Pérez-Marín, Hyperspectral Imaging for the detection of bitter almonds in sweet almond batches, Appl. Sci. 12 (2022) 4842, https://doi.org/10.3390/app12104842.
[82] M.A. Faqeerzada, S. Lohumi, G. Kim, R. Joshi, H. Lee, M.S. Kim, B.K. Cho, Hyperspectral shortwave infrared image analysis for detection of adulterants in almond powder with one-class classification method, Sensors 20 (2020) 5855, https://doi.org/10.3390/s20205855.
[83] I. Orrillo, J.P. Cruz-Tirado, A. Cardenas, M. Oruna, A. Carnero, D.F. Barbin, R. Siche, Hyperspectral imaging as a powerful tool for identification of papaya seeds in black pepper, Food Control 101 (2019) 45–52, https://doi.org/10.1016/j.foodcont.2019.02.036.
[84] X. Li, H. Jiang, X. Jiang, M. Shi, Identification of geographical origin of Chinese chestnuts using hyperspectral imaging with 1D-CNN algorithm, Agriculture 11 (2021) 1274, https://doi.org/10.3390/agriculture11121274.
[85] J.P. Cruz-Tirado, Y.L. Brasil, A.F. Lima, H.A. Pretel, H.T. Godoy, D. Barbin, R. Siche, Rapid and non-destructive cinnamon authentication by NIR-hyperspectral imaging and classification chemometrics tools, Spectrochim Acta A Mol Biomol Spectrosc. 289 (2023) 122226, https://doi.org/10.1016/j.saa.2022.122226.
[86] M. Aqeel, A. Sohaib, M. Iqbal, H.U. Rehman, F. Rustam, Hyperspectral identification of oil adulteration using machine learning techniques, Curr Res Food Sci. 8 (2024) 100773, https://doi.org/10.1016/j.crfs.2024.100773.
[87] D. Malavi, K. Raes, S. Van Haute, Integrating Near-Infrared hyperspectral imaging with machine learning and feature selection: detecting adulteration of extra-virgin olive oil with lower-grade olive oils and hazelnut oil, Curr Res Food Sci. 9 (2024) 100913, https://doi.org/10.1016/j.crfs.2024.100913.
[88] B. Borràs-Vallverdú, S. Marín, V. Sanchis, F. Gatius, A.J. Ramos, NIR-HSI as a tool to predict deoxynivalenol and fumonisins in maize kernels: a step forward in preventing mycotoxin contamination, J Sci Food Agric. 104 (2024) 5495–5503, https://doi.org/10.1002/jsfa.13388.
[89] Z. Wang, T. An, W. Wang, S. Fan, L. Chen, X. Tian, Qualitative and quantitative detection of aflatoxins B1 in maize kernels with fluorescence hyperspectral imaging based on the combination method of boosting and stacking, Spectrochim Acta A Mol Biomol Spectrosc. 296 (2023) 122679, https://doi.org/10.1016/j.saa.2023.122679.
[90] S.K. Chakraborty, N.K. Mahanti, S.M. Mansuri, M.K. Tripathi, N. Kotwaliwale, D. S. Jayas, Non-destructive classification and prediction of aflatoxin-B1 concentration in maize kernels using Vis–NIR (400–1000 nm) hyperspectral imaging, J Food Sci Technol. 58 (2021) 437–450, https://doi.org/10.1007/s13197-020-04552-w.
[91] V. Parrag, Z. Gillay, Z. Kovács, A. Zitek, K. Böhm, B. Hinterstoisser, L. Baranyai, Application of hyperspectral imaging to detect toxigenic Fusarium infection on cornmeal, Prog Agric Eng Sci. 16 (2020) 51–60, https://doi.org/10.1556/446.2020.00009.
[92] D. Wu, L. Meng, L. Yang, J. Wang, X. Fu, X. Du, L. Huang, Feasibility of laser-induced breakdown spectroscopy and hyperspectral imaging for rapid detection of thiophanate-methyl residue on mulberry fruit, Int J Mol Sci. 20 (2019) 2017, https://doi.org/10.3390/ijms20082017.
[93] V. Ferrari, R. Calvini, C. Menozzi, A. Ulrici, M. Bragolusi, R. Piro, G. Foca, Addressing adulteration challenges of dried oregano leaves by NIR HyperSpectral Imaging, Chemom Intell Lab Syst. 249 (2024) 105133, https://doi.org/10.1016/j.chemolab.2024.105133.

[94] C. Nie, J. Jiang, Z. Liu, D. Yuan, K. Li, M. Li, Detecting moldy peanuts via moldiness index and kernel features by hyperspectral imaging, J Food Meas Charact. 18 (2024) 1857–1877, https://doi.org/10.1007/s11694-023-02300-0.
[95] Z. Izadi, S. Kiani, Pomegranate molasses authentication using hyperspectral imaging system coupled with automatic clustering algorithm, J Food Sci. 89 (2024) 4216–4228, https://doi.org/10.1111/1750-3841.17134.
[96] R. Ríos-Reina, R.M. Callejón, J.M. Amigo, Feasibility of a rapid and non-destructive methodology for the study and discrimination of pine nuts using near-infrared hyperspectral analysis and chemometrics, Food Control 130 (2021) 108365, https://doi.org/10.1016/j.foodcont.2021.108365.
[97] S. Weng, P. Tang, H. Yuan, B. Guo, S. Yu, L. Huang, C. Xu, Hyperspectral imaging for accurate determination of rice variety using a deep learning network with multi-feature fusion, Spectrochim Acta A Mol Biomol. Spectrosc. 234 (2020) 118237, https://doi.org/10.1016/j.saa.2020.118237.
[98] U. Siripatrawan, Y. Makino, Assessment of food safety risk using machine learning-assisted hyperspectral imaging: Classification of fungal contamination levels in rice grain, Microb Risk Anal. 27 (2024) 100295, https://doi.org/10.1016/j.mran.2024.100295.
[99] Z. Fa Wang, G. Chen, R. Jiang, M. Zhao, T. Lin, R. Wang, J. Wang, SC-HybridSN: A deep learning network method for rapid discriminant analysis of industrial paraffin contamination levels in rice, J Food Compos. Anal. 133 (2024) 106404, https://doi.org/10.1016/j.jfca.2024.106404.
[100] D. Malavi, A. Nikkhah, P. Alighaleh, S. Einafshar, K. Raes, S. Van Haute, Detection of saffron adulteration with Crocus sativus style using NIR-hyperspectral imaging and chemometrics, Food Control 157 (2024) 110189, https://doi.org/10.1016/j.foodcont.2023.110189.
[101] F.S. Hashemi-Nasab, H. Parastar, Vis-NIR hyperspectral imaging coupled with independent component analysis for saffron authentication, Food Chem. 393 (2022) 133450, https://doi.org/10.1016/j.foodchem.2022.133450.
[102] C.D. Everard, M.S. Kim, H.A. Lee, Comparison of hyperspectral reflectance and fluorescence imaging techniques for detection of contaminants on spinach leaves, J Food Eng. 143 (2014) 139–145, https://doi.org/10.1016/j.jfoodeng.2014.06.042.
[103] Z. Bai, X. Hu, J. Tian, P. Chen, H. Luo, D. Huang, Rapid and nondestructive detection of sorghum adulteration using optimization algorithms and hyperspectral imaging, Food Chem. 331 (2020) 127290, https://doi.org/10.1016/j.foodchem.2020.127290.
[104] P. Mishra, A. Nordon, J. Tschannerl, G. Lian, S. Redfern, S. Marshall, Near-infrared hyperspectral imaging for non-destructive classification of commercial tea products, J Food Eng. 238 (2018) 70–77, https://doi.org/10.1016/j.jfoodeng.2018.06.015.
[105] L. Zheng, Q. Bao, S. Weng, J. Tao, D. Zhang, L. Huang, J. Zhao, Determination of adulteration in wheat flour using multi-grained cascade forest-related models coupled with the fusion information of hyperspectral imaging, Spectrochim Acta A Mol Biomol. Spectrosc. 270 (2022) 120813, https://doi.org/10.1016/j.saa.2021.120813.
[106] A. Nirere, J. Sun, R. Kama, V.A. Atindana, F.D. Nikubwimana, K.D. Dusabe, Y. Zhong, Nondestructive detection of adulterated wolfberry (Lycium Chinense) fruits based on hyperspectral imaging technology, J Food Process Eng. 46 (2023) 14293, https://doi.org/10.1111/jfpe.14293.
[107] Y. Zhang, Y. Li, C. Zhou, J. Zhou, T. Nan, J. Yang, L. Huang, Rapid and nondestructive identification of origin and index component contents of Tiegun yam based on hyperspectral imaging and Chemometric method, J. Food Qual. 1 (2023) 6104038, https://doi.org/10.1155/2023/6104038.